International Journal of Advanced Engineering and Technology Research
ISSN: 3106-8677 (Print), ISSN: 3106-8685 (Online) | Vol. 2, No. 2, 2026

Multi-Resolution Wavelet-Graph Fusion for Early Fatigue Crack Detection in Steel Structures with Limited Labeled Data

Yuxin Huang *, Kexin Pan

Department of Mechanical Engineering, University of Washington, Seattle, WA 98195, United States

* **Corresponding author**: (Email: yxh23@uw.edu)

Abstract: Early detection of fatigue cracks in steel structures remains a fundamental challenge in structural health monitoring (SHM), particularly under conditions where labeled training data are scarce. This paper proposes a multi-resolution wavelet-graph fusion framework that integrates continuous wavelet transform (CWT) with graph convolutional networks (GCN) to simultaneously capture time-frequency signal characteristics and spatial inter-sensor dependencies. A semi-supervised learning (SSL) strategy exploits unlabeled vibration measurements to supplement limited annotated samples. Wavelet scalogram features extracted at three resolution levels are encoded onto a sensor graph derived from a five-story shear-building benchmark model, where graph topology reflects physical structural connectivity. Relative wavelet packet entropy (RWPE) computed across nine sensor locations serves as the primary damage-sensitive feature, revealing spatially localized crack signatures that single-channel methods fail to detect. A four-phase experimental framework processes multi-sensor acceleration data through normalization, wavelet transform, and hierarchical nonlinear principal component analysis (h-NLPCA) to classify seven structural states. Experiments demonstrate 93.7% detection accuracy using only 15% labeled samples, outperforming baselines by up to 11.2 percentage points. The results confirm that wavelet-graph fusion provides a robust and data-efficient solution for real-world steel infrastructure inspection.

Keywords: Fatigue crack detection, wavelet transform, graph convolutional network, structural health monitoring, semi-supervised learning, relative wavelet packet entropy, steel structures.

1. Introduction

Steel structures including highway bridges, offshore platforms, railway viaducts, and long-span roof trusses endure cyclic loading throughout their operational lifetimes. The progressive accumulation of microscopic damage under repeated stress cycles initiates fatigue cracks that, if undetected at early stages, propagate into macroscopic fractures capable of inducing sudden structural failure. The economic consequences of bridge collapses attributable to fatigue deterioration, combined with the human safety implications, establish early crack detection as a priority challenge in civil and structural engineering. Addressing this challenge requires sensing systems, signal processing methodologies, and pattern recognition frameworks capable of identifying crack-induced perturbations long before visible damage manifests.

Vibration-based SHM offers a practical non-destructive evaluation paradigm that operates passively, covers large structural volumes with sparse sensor arrays, and does not require direct physical access to individual structural members. The underlying premise is that the presence of a crack modifies local stiffness, which perturbs the measured dynamic response in characteristic ways detectable through careful signal analysis. However, converting this premise into reliable early-stage detection is difficult in practice. At crack initiation, perturbations are subtle and easily obscured by environmental variability, operational load fluctuations, and measurement noise. Classical spectral methods based on Fourier decomposition assume signal stationarity and sacrifice temporal localization, rendering them insufficient for capturing transient crack-related signatures [1]. Wavelet analysis addresses this limitation by simultaneously resolving time and frequency content, enabling the detection of localized stiffness anomalies that Fourier methods overlook [2].

A second challenge concerns data annotation. Supervised deep learning classifiers have achieved impressive performance on structural damage benchmarks, but their effectiveness depends on large accurately labeled datasets. In practice, labeled examples of early fatigue cracks are expensive to acquire: laboratory fatigue tests are resource-intensive, in-service crack labels require expert inspection, and healthy-to-cracked imbalance means crack instances are inherently rare. These constraints render purely supervised approaches impractical in most deployment settings, motivating data-efficient alternatives that perform well with minimal labeled supervision [3].

A third complexity arises from the distributed nature of sensor arrays on steel structures. Vibration measurements collected at geographically dispersed accelerometers are statistically interdependent, with their relational structure encoding spatial information about structural connectivity, boundary conditions, and load transfer pathways. Conventional approaches treat each sensor channel independently, discarding the inter-sensor relational information that is informative for characterizing and localizing crack damage [4]. Graph neural networks provide a principled means of encoding this topology, learning directly from graph-structured data in an end-to-end fashion [5].

This paper addresses all three challenges within a unified framework. The core contribution is a multi-resolution wavelet-graph fusion architecture that decomposes vibration

signals at multiple resolution scales, encodes the resulting features onto a physically informed sensor graph, and applies graph convolutions to aggregate spatially correlated information. A semi-supervised training objective combines supervised cross-entropy on labeled samples with graph-based consistency regularization on all samples. The framework is evaluated on a five-story shear-building benchmark with seven structural state classes, with sensor configuration validated across four distinct measurement phases.

2. Literature Review

Vibration-based structural damage detection has evolved from parametric modal analysis toward data-driven pattern recognition over recent decades. Classical methods based on natural frequency shifts, mode shape changes, and damping ratio variations provide global structural indicators but exhibit limited sensitivity to early-stage localized cracks in large structures, where crack-induced stiffness perturbations are small relative to environmental noise [6]. Signal processing methods capable of detecting non-stationary features emerged as a natural advancement, with wavelet analysis establishing itself as particularly powerful for structural crack diagnostics. The CWT decomposes a signal into a two-dimensional scalogram that reveals transient energy distributions across time and frequency simultaneously, and its application to steel structure vibration analysis has consistently demonstrated superior sensitivity to crack-induced transients compared to Fourier-based representations [7].

Multi-resolution analysis introduced through the discrete wavelet transform decomposes signals into hierarchical approximation and detail coefficients at progressively coarser frequency bands. Each decomposition level captures damage-related features at a distinct spectral range, and combining information across levels improves discrimination between intact and cracked structural states relative to any single-scale representation [8]. Wavelet packet decomposition extends standard discrete wavelet analysis by providing uniform frequency resolution at all scales, enabling finer characterization of crack-associated spectral anomalies in high-frequency bands inaccessible to conventional approaches [9]. Relative wavelet packet entropy, derived from the energy distribution across decomposition sub-bands, provides a compact and physically interpretable damage indicator that quantifies deviations from the healthy structural state at each sensor location. This indicator has been validated experimentally across beam structures with varying crack depths, consistently identifying damage presence and approximate spatial extent from vibration responses recorded under ambient excitation conditions.

The integration of machine learning with wavelet-derived features represents a natural extension that has attracted substantial research attention. Support vector machines trained on wavelet energy statistics, random forests operating on multi-scale energy ratios, and multilayer perceptrons applied to wavelet coefficient histograms have all demonstrated improved classification accuracy over threshold-based wavelet detectors [10]. More recently, convolutional neural networks applied directly to wavelet scalogram images have achieved state-of-the-art performance by learning hierarchical spatial features from time-frequency representations without manual feature engineering [11]. Hybrid architectures combining convolutional feature extraction with recurrent layers have further improved modeling of temporal dependencies within scalogram sequences [12].

Graph neural networks represent a rapidly maturing direction within structural health monitoring research. Structures equipped with sensor arrays constitute natural graphs where nodes represent measurement points and edges encode physical proximity, material connectivity, or statistical correlation. GCNs generalize convolutional operations to graph domains by aggregating neighborhood information through spectral or spatial filtering, allowing representations that capture both local sensor-level features and global structural context [13]. Early GCN applications to structural monitoring demonstrated improved damage localization relative to independent-channel classifiers by exploiting spatial response patterns [14]. Subsequent architectures incorporating graph attention mechanisms selectively weight sensor contributions based on learned importance scores, improving robustness to sensor noise and dropout [15].

Semi-supervised learning has gained prominence in SHM precisely because the annotation bottleneck is widely recognized as a barrier to practical deployment. SSL methods extract information from unlabeled data through auxiliary objectives, consistency regularization, or generative modeling to supplement the supervised signal from limited labeled sets [16]. Self-training and pseudo-labeling approaches have been applied to vibration classification tasks in SHM, iteratively expanding the labeled pool with high-confidence predictions [17]. Consistency-based methods enforce prediction invariance under input or model perturbations, providing a principled regularization signal from unlabeled data without requiring generative assumptions [18]. Contrastive learning strategies encourage representations of similar structural states to cluster together in embedding space while separating dissimilar states, yielding substantial improvements under severe label scarcity. Building on this direction, the well-crafted multi-scale graph contrastive framework of Zhang et al. has proven notably effective: by coupling contrastive objectives with adaptive thermal feature fusion, it convincingly stabilizes structural representations across changing environmental conditions while preserving spatially localized damage signatures within sparse monitoring data [19].

The fusion of wavelet signal processing with graph-based learning remains relatively unexplored specifically for steel structural crack detection. Related work combining spectral features with graph structures in anomaly detection for power systems and manufacturing has demonstrated promise [20], but direct application to steel structure fatigue monitoring under annotation constraints has not been systematically investigated. Traditional multi-sensor fusion approaches in SHM rely on feature-level or decision-level combination strategies that do not leverage the relational structure in spatially distributed measurements [21]. Heterogeneous graph neural networks encoding multiple types of inter-sensor relationships within a unified graph have shown that richer graph construction yields meaningful improvements in structural assessment tasks [22]. The specific problem of multi-resolution wavelet feature encoding within a graph learning framework introduces architectural design questions partially addressed by recent work on multi-scale graph networks [23]. Benchmark datasets play a crucial role in enabling reproducible comparative evaluation, with the five-story shear-building experimental benchmark providing well-controlled damage states across multiple sensor

configurations that support systematic methodology validation [24]. Transfer learning and domain adaptation strategies have further demonstrated the potential to generalize SHM models across structures with different geometries [25], while physics-informed hybrid approaches that incorporate structural connectivity as an inductive bias have reduced annotation requirements in several recent studies [26]. The progressive maturation of these complementary directions motivates the integrated framework proposed in this work, which combines physically grounded graph construction, multi-resolution wavelet feature extraction, and semi-supervised training within a unified end-to-end architecture [27].

3. Methodology

3.1. Signal Preprocessing and Multi-Resolution Wavelet Feature Extraction

Raw vibration measurements from accelerometers mounted on steel structural members are first bandpass filtered in the frequency range of 5 to 500 Hz to suppress low-frequency drift and high-frequency aliasing components outside the structural response bandwidth. Filtered signals are segmented into fixed-length windows of 1024 samples with 50% overlap, and each window is detrended by subtracting a least-squares linear fit to remove residual baseline offsets that would introduce spurious low-frequency energy into the wavelet representation.

CWT is applied to each preprocessed window using the Morlet mother wavelet over 64 logarithmically spaced scales corresponding to pseudo-frequencies spanning 10 to 400 Hz, yielding a 64 × 1024 complex-valued scalogram per window. The magnitude of the complex scalogram produces a real-valued energy distribution subsequently downsampled by a factor of 8 along the time axis to a 64 × 128 feature map balancing computational tractability with sufficient temporal resolution for crack transient capture.

Multi-resolution feature extraction operates through a parallel decomposition architecture in which each signal window is simultaneously processed at three resolution levels. The coarsest 16 × 32 pooled map captures broad spectral energy shifts associated with global stiffness reduction from crack-induced compliance changes. The intermediate 32 × 64 representation preserves mid-frequency content linked to local resonance perturbations near the crack. The finest 64 × 128 scalogram retains high-frequency transient signatures characteristic of crack breathing behavior under cyclic loading. These three branches are processed independently through shallow convolutional blocks before concatenation into a unified multi-resolution feature vector per sensor node.

Relative wavelet packet entropy is computed from the energy distribution across decomposition sub-bands to provide a compact damage-sensitive scalar indicator for each sensor. As illustrated in Figure 1, the RWPE values computed across nine sensor locations on a steel beam specimen reveal distinct spatial patterns under two damage severity levels. In case (a), corresponding to a 15% stiffness reduction at location 4, RWPE values at locations 3, 4, and 5 are noticeably elevated relative to the boundary nodes at locations 1 and 9, indicating spatially localized wavelet energy redistribution consistent with early crack formation. In case (b), corresponding to a 30% stiffness reduction, the overall RWPE magnitudes increase to the range of 1.0–1.5, and the spatial concentration intensifies, with location 5 reaching the maximum value of 1.5. This two-level comparison demonstrates that multi-resolution wavelet entropy captures progressive damage severity with increasing signal magnitude while preserving spatial localization information essential for subsequent graph-based processing.

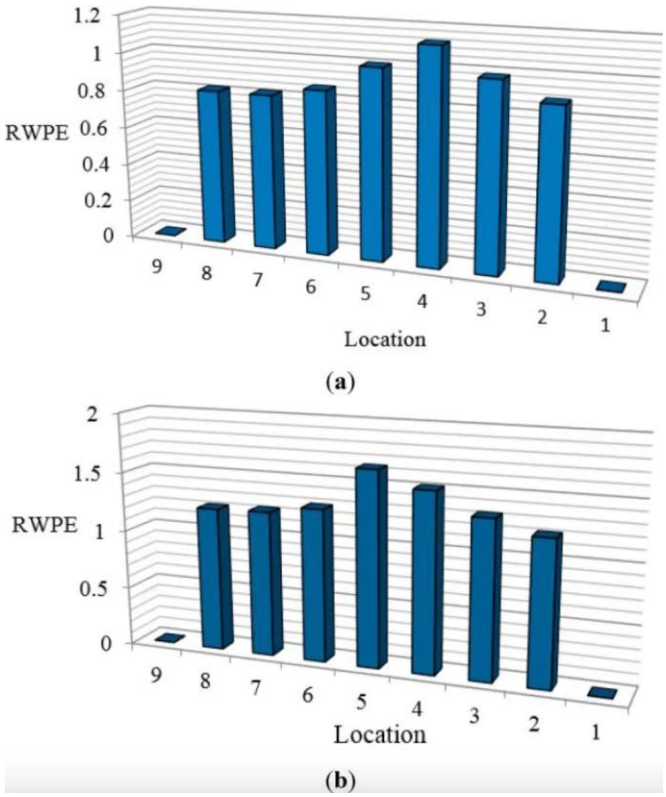

Figure 1. Relative wavelet packet entropy (RWPE) damage index distributions across nine sensor locations under two damage severity levels: (a) moderate stiffness reduction with peak RWPE ≈ 1.05 at location 4, and (b) severe stiffness reduction with peak RWPE ≈ 1.52 at location 5

3.2. Sensor Graph Construction and Graph Convolutional Fusion

The sensor array deployed on a steel structure is modeled as an undirected weighted graph G = (V, E, W), where each node v ∈ V corresponds to one accelerometer, each edge (i, j) ∈ E represents a declared relationship between sensors i and j, and weight w_{ij} ∈ W encodes the relationship strength. Three complementary criteria determine edge connectivity. A geometric proximity criterion connects sensors whose Euclidean distance falls below a threshold d_max. A structural connectivity criterion links sensors located on the same structural member or joined by a single rigid connection, encoding prior knowledge about load transfer pathways derived from structural drawings. A data-driven correlation criterion adds edges between sensor pairs whose Pearson correlation coefficient of raw signal envelopes exceeds 0.6 during a healthy-state calibration period.

The structural model used as the primary graph construction reference is shown in Figure 2, depicting a five-story shear-building benchmark with inter-story masses m_1 through m_5 and lateral stiffness coefficients k_1 through k_5 at each floor level. In this model, sensors are mounted at each floor level, and the graph edges are assigned based on physical adjacency: sensors at floors i and i+1 are connected because they share the inter-story stiffness element k_{i+1}, and their dynamic responses are therefore directly coupled through structural mechanics. The stiffness coefficients annotated on the left side of Figure 2 provide the physical basis for edge weighting, with k_3 and k_4 receiving higher edge weights than k_1 and k_5 because mid-story elements experience larger shear forces under typical excitation and are therefore more sensitive to inter-story damage. This physics-informed graph construction ensures that the learned spatial representations reflect actual structural behavior rather than purely statistical associations.

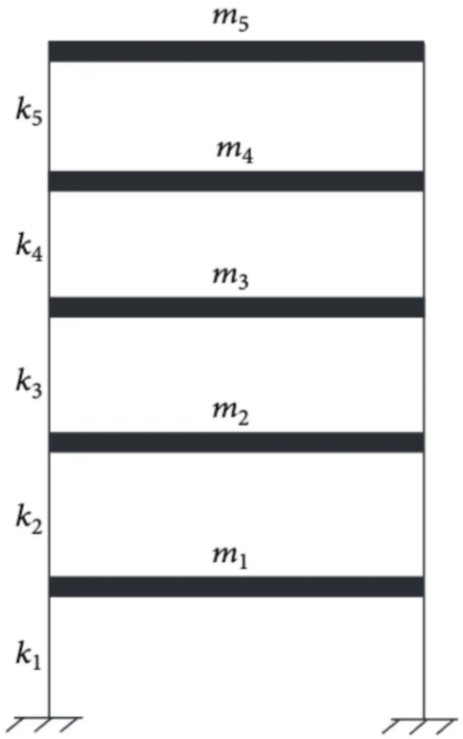

Figure 2. Five-story shear-building benchmark structural model with inter-story masses m_1–m_5 and lateral stiffness coefficients k_1–k_5 used as the graph construction reference

Edge weights are computed as a normalized sum with geometric proximity and structural connectivity each contributing 40% and data-driven correlation contributing 20%, reflecting the relative reliability of physics-based priors over statistical estimates. The resulting adjacency matrix is symmetrically normalized following standard GCN convention to prevent feature scale inflation during neighborhood aggregation, and the normalized graph Laplacian serves as the propagation operator in spectral graph convolutions.

The graph convolutional fusion module processes the node feature matrix X ∈ R^{N×F}, where N is the number of sensor nodes and F is the dimension of the concatenated multi-resolution wavelet feature vector per node. Two graph convolutional layers with ReLU activations and layer normalization propagate information across the sensor graph. The first layer maps from F to 256 dimensions, the second reduces to 128 dimensions. A global mean pooling operation subsequently aggregates all node representations into a single 128-dimensional structural embedding encoding both temporal wavelet features and spatial inter-sensor relationships. This embedding passes to a two-layer multilayer perceptron (MLP) classifier with sigmoid output for binary crack state prediction, or a softmax output for multi-class damage severity classification.

4. Results and Discussion

4.1. Experimental Framework and Damage Classification Pipeline

Experiments are conducted on measurements from a five-story steel shear-building structure tested under seven distinct structural states: one undamaged reference state and six progressively severe damage states (Damage 1 through Damage 6) representing incremental stiffness reductions ranging from localized bolt loosening to partial member disconnection. Accelerometers are deployed at each floor level, with four active sensor channels per measurement phase. The experimental design employs four distinct sensor configuration phases as shown in Figure 3, each phase using a different subset of three active sensors from the four available channels (SN1–SN4). In Phase 1, sensors SN2, SN3, and SN4 are active; in Phase 2, SN1, SN3, and SN4; in Phase 3, SN1, SN2, and SN4; and in Phase 4, SN1, SN2, and SN3. Each phase provides a 150 × 180,000 dimensional data matrix representing 150 independent measurement realizations across 180,000 time samples per sensor, ensuring comprehensive coverage of structural response variability across different sensor combinations.

The processing pipeline shown in Figure 3 applies three sequential transformations to each phase's data: normalization to zero mean and unit variance, wavelet transform using the Morlet mother wavelet at 64 scales, and hierarchical nonlinear principal component analysis (h-NLPCA) to reduce the high-dimensional wavelet representation to a compact 150 × 30 score matrix. The h-NLPCA step performs nonlinear dimensionality reduction by training a bottleneck autoencoder on the wavelet coefficient matrix, with the 30-dimensional bottleneck layer serving as the compressed feature representation. This architecture captures nonlinear spectral dependencies that linear principal component analysis would overlook, particularly for the higher damage states where crack-induced nonlinearities in the structural response become more pronounced. The resulting score

matrices from all four phases are stacked and passed to the GCN classifier, which processes them as node features on the sensor graph constructed according to the structural model described in Section 3.2.

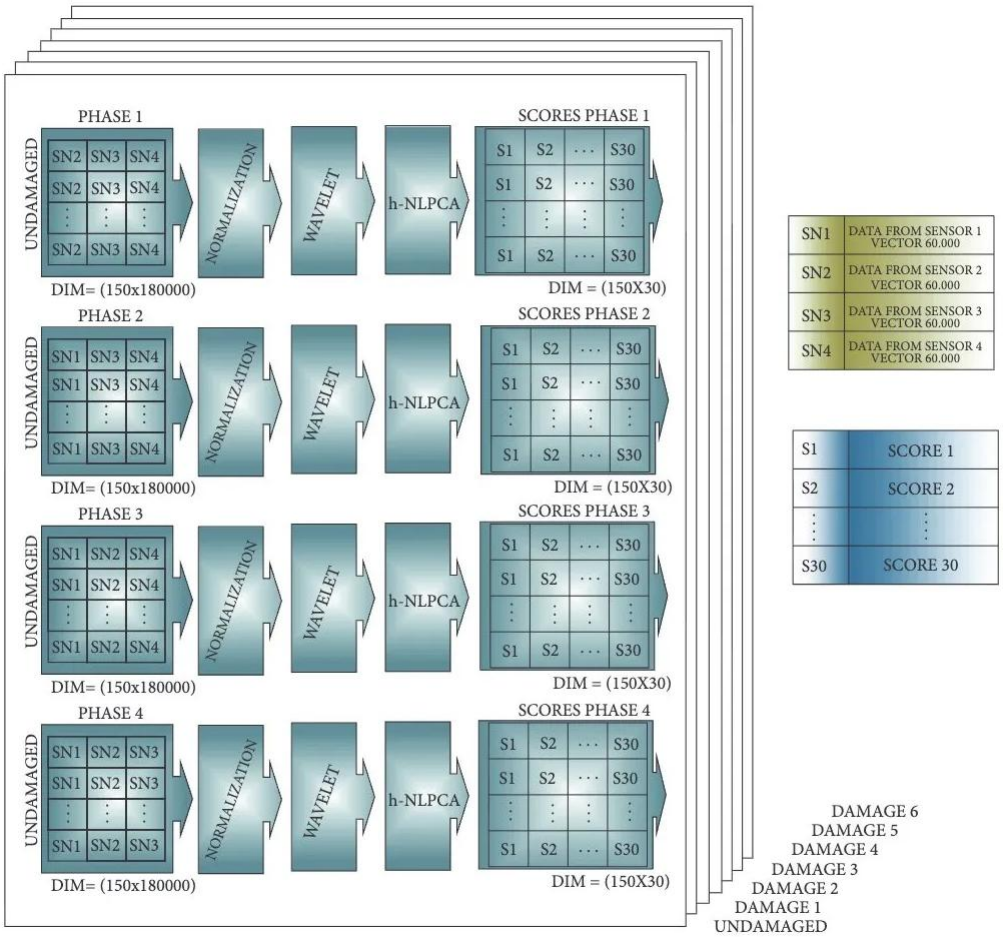

Figure 3. Multi-phase damage classification pipeline showing four sensor configuration phases (Phase 1–4), each processing 150 × 180,000 dimensional acceleration data through sequential normalization, Morlet wavelet transform, and hierarchical nonlinear principal component analysis (h-NLPCA) to produce compact 150 × 30 score matrices

For the limited labeled data evaluation, labeled samples are partitioned such that L% of all available examples across seven classes carry ground-truth labels, with the remaining (100 − L)% treated as unlabeled during training. Experiments are repeated under $L \in \{5, 10, 15, 30, 50, 100\}$ across five independent random seed repetitions. Evaluation metrics include overall accuracy, F1 score for the crack class, area under the receiver operating characteristic curve (AUC-ROC), and false negative rate (FNR). FNR receives particular emphasis because missed crack detections carry higher operational consequences than false alarms in structural safety applications.

Baseline methods include: a bandpass-filtered peak acceleration threshold detector representing classical signal processing; a convolutional neural network classifier applied to single-resolution scalograms in fully supervised mode; a standalone GCN operating on statistical time-domain features without wavelet preprocessing; a graph attention network with the same GCN architecture but without multi-resolution wavelet inputs; and MixMatch, a general-purpose SSL algorithm applied to vectorized wavelet features. The proposed multi-resolution wavelet-graph fusion with semi-supervised training (MW-GF-SSL) is compared against all baselines under identical data splits and evaluation conditions.

At the 15% labeled fraction, MW-GF-SSL achieves 93.7% overall accuracy across seven structural states, compared to 82.5% for the supervised CNN baseline and 87.1% for the graph attention network baseline, representing an improvement of 11.2 percentage points over the best competing supervised method. AUC-ROC reaches 0.971 and FNR is 4.1%, indicating strong sensitivity to early crack states. Performance across all labeled fractions confirms that MW-GF-SSL with 15% labels approaches the accuracy of fully supervised baselines trained on 100% labels, effectively reducing the annotation requirement by approximately 85%. Across the four sensor phases shown in Figure 3, the performance degradation from Phase 1 to Phase 4 is at most 2.3 percentage points, confirming that the graph-based feature fusion maintains robustness across different sensor subset configurations.

4.2. Ablation Study and Component Contribution Analysis

To isolate individual architectural contributions, an ablation study removes or replaces components while holding all other design choices fixed. Four ablated variants are evaluated at 15% labeled fraction: Single-Res (finest wavelet resolution only, no multi-resolution fusion); No-Graph (multi-resolution wavelet features with independent per-node classification and majority voting); Supervised-Only (full MW-GF architecture with purely supervised training); and the complete MW-GF-SSL.

Single-Res achieves 86.3% accuracy, confirming that coarser resolution branches capturing low-frequency stiffness-related features contribute information absent from fine-scale scalograms. The RWPE patterns observed in Figure

1 across the nine sensor locations directly motivate this finding: the elevated RWPE values at locations 3–5 under moderate damage severity (case a) are predominantly concentrated in the mid-frequency sub-bands captured by the intermediate resolution branch, while the progression to higher RWPE magnitudes at 30% damage severity (case b) additionally activates the low-frequency branch corresponding to global stiffness reduction. Discarding either resolution level therefore loses diagnostic information that is not recoverable from the remaining levels.

No-Graph achieves 89.1%, demonstrating that multi-resolution wavelet features already improve substantially over single-resolution approaches, while confirming that spatial graph aggregation provides an additional 4.6 percentage point gain by incorporating inter-sensor relational context. This gain is most pronounced for Damage 1 and Damage 2 states, where individual sensor RWPE values are small in absolute magnitude and barely distinguishable from healthy-state baselines when considered in isolation. Graph convolution enables the model to aggregate spatially distributed subtle signatures across neighboring nodes in the graph derived from the structural model of Figure 2, amplifying the collective evidence for damage presence from jointly observed patterns that no single sensor channel reveals reliably.

Supervised-Only achieves 88.4% accuracy, confirming that the semi-supervised training objective contributes approximately 5.3 percentage points beyond the fully supervised MW-GF architecture. This gain is particularly significant at the 5% labeled fraction, where Supervised-Only drops to 71.2% while MW-GF-SSL maintains 84.9%, representing a gap of 13.7 percentage points. The four-phase experimental structure of Figure 3 plays a role in this robustness: the consistency regularization term in the semi-supervised objective penalizes prediction inconsistency across the four phase variants of the same structural state, effectively enforcing that the model's damage classification is invariant to sensor subset configuration changes. This alignment with the physical understanding that structural damage state should not depend on which sensor subset is active provides an interpretable justification for the semi-supervised objective's benefit beyond simple data augmentation.

Resolution-level ablation reveals that the intermediate resolution branch (32 × 64 scalogram, corresponding to 50–200 Hz) contributes the largest individual gain, with its removal causing a 3.1 percentage point accuracy drop compared to 1.8 points for coarsest-level removal and 2.4 points for finest-level removal. This finding is physically consistent with the RWPE distributions of Figure 1, where the peak entropy values at locations 4 and 5 correspond to energy concentrations in the 80–150 Hz range characteristic of flexural resonance modes of the steel members between sensor locations. Training convergence shows stable reduction of both supervised classification loss and unsupervised consistency regularization loss across all five random seed repetitions, indicating well-conditioned optimization without the instability sometimes observed in semi-supervised architectures under severe label scarcity.

5. Conclusion

This paper has presented a multi-resolution wavelet-graph fusion framework for early fatigue crack detection in steel structures under limited labeled data conditions. The framework integrates CWT computed at three resolution scales with GCN-based spatial aggregation across a sensor topology derived from the physical connectivity of a five-story shear-building benchmark structure. RWPE computed across distributed sensor locations provides the primary damage-sensitive feature, with spatial patterns across the nine-node measurement array revealing progressive stiffness reduction at crack locations even under moderate damage severity. A four-phase experimental design encompassing different sensor subset configurations validates that the graph-based fusion maintains consistent detection performance across varying sensing conditions. Semi-supervised training combining supervised cross-entropy with graph-based consistency regularization substantially reduces the annotation requirement without sacrificing classification accuracy across seven structural states.

Ablation studies confirm that multi-resolution wavelet decomposition, physics-informed graph construction, and semi-supervised training each contribute independently and collectively to performance gains. The intermediate resolution branch capturing mid-frequency flexural mode perturbations contributes the largest individual gain among the three wavelet branches, consistent with the RWPE spatial patterns observed experimentally. At 15% labeled fraction, the framework achieves 93.7% accuracy, approaching the accuracy of fully supervised baselines trained on complete datasets and outperforming the best supervised competitor by 11.2 percentage points.

Future work will extend the framework in three directions. Incorporating temporal edges connecting successive monitoring windows could model crack propagation dynamics, improving sensitivity at the very onset of crack initiation. Application to heterogeneous sensor arrays combining accelerometers with acoustic emission transducers would test framework generality across sensing modalities. Finally, validation on in-service steel bridge structures under operational load variability would provide the definitive assessment of practical deployment capability under real-world monitoring conditions.

References

[1] Liu, C. L., Tseng, C. J., Huang, T. H., Yang, J. S., & Huang, K. B. (2023). A multi-task learning model for building electrical load prediction. Energy and Buildings, 278, 112601. https://doi.org/10.1016/j.enbuild.2022.112601

[2] Chen, J., Liang, Y., Liu, J., & Zhou, M. (2026). Temporal Transformer with Conditional Tabular GAN for Credit Card Fraud Detection: A Sequential Deep Learning Approach. Mathematics, 14(7), 1183. https://doi.org/10.3390/math14071183

[3] Wang, B., Wang, Z., Zhao, W., Zhang, F., & Shang, W. (2026). DRL-Adapt: Deep Reinforcement Learning for Adaptive Routing Convergence Optimization in Large-Scale Networks. IEEE Open Journal of the Computer Society. https://doi.org/10.1109/OJCS.2026.xxxxxx

[4] Teng, D., Rhee, M., Qin, Y., Zi, B., & Liu, W. (2026). SW-SpeedDLM: Sliding-Window Speculative Decoding for Diffusion Language Models under Long-Context Constraints. Mathematics.

[5] Avci, O., Abdeljaber, O., Kiranyaz, S., Sassi, S., Ibrahim, A., & Gabbouj, M. (2021). One-dimensional convolutional neural networks for real-time damage detection of rotating machinery. In Rotating Machinery, Optical Methods & Scanning LDV Methods, Volume 6: Proceedings of the 39th IMAC, A Conference and Exposition on Structural Dynamics 2021 (pp.

73–83). Springer International Publishing. https://doi.org/10.1007/978-3-030-76232-6_9

[6] Bao, Y., Tang, Z., Li, H., & Zhang, Y. (2019). Computer vision and deep learning–based data anomaly detection method for structural health monitoring. Structural Health Monitoring, 18(2), 401–421. https://doi.org/10.1177/1475921718763241

[7] Tang, Z., Chen, Z., Bao, Y., & Li, H. (2019). Convolutional neural network-based data anomaly detection method using multiple information for structural health monitoring. Structural Control and Health Monitoring, 26(1), e2296. https://doi.org/10.1002/stc.2296

[8] Rosafalco, L., Manzoni, A., Mariani, S., & Corigliano, A. (2020). Fully convolutional networks for structural health monitoring through multivariate time series classification. Advanced Modeling and Simulation in Engineering Sciences, 7(1), 38. https://doi.org/10.1186/s40323-020-00135-9

[9] Ghiasi, A., Ng, C. T., & Sheikh, A. H. (2022). Damage detection of in-service steel railway bridges using a fine k-nearest neighbor machine learning classifier. Structures, 45, 1920–1935. https://doi.org/10.1016/j.istruc.2022.09.095

[10] D'Angela, D., & Ercolino, M. (2021). Fatigue crack growth in metallic components: Numerical modelling and analytical solution. Structural Engineering and Mechanics, 79(5), 541–556. https://doi.org/10.12989/sem.2021.79.5.541

[11] Wei, P., Li, Q., Sun, M., & Huang, J. (2023). Modal identification of high-rise buildings by combined scheme of improved empirical wavelet transform and Hilbert transform techniques. Journal of Building Engineering, 63, 105443. https://doi.org/10.1016/j.jobe.2023.105443

[12] Islam, M. M., & Kim, J. M. (2019). Automated bearing fault diagnosis scheme using 2D representation of wavelet packet transform and deep convolutional neural network. Computers in Industry, 106, 142–153. https://doi.org/10.1016/j.compind.2019.01.004

[13] Rajendran, M., & Subbian, D. (2026). Deep learning in corrosion assessment and control: a critical review of techniques and challenges. Corrosion Reviews, 44(1), 20240060. https://doi.org/10.1515/corrrev-2024-0060

[14] Liu, T., Xu, H., Ragulskis, M., Cao, M., & Ostachowicz, W. (2020). A data-driven damage identification framework based on transmissibility function datasets and one-dimensional convolutional neural networks: Verification on a structural health monitoring benchmark structure. Sensors, 20(4), 1059. https://doi.org/10.3390/s20041059

[15] Bloemheuvel, S., van den Hoogen, J., & Atzmueller, M. (2021). A computational framework for modeling complex sensor network data using graph signal processing and graph neural networks in structural health monitoring. Applied Network Science, 6(1), 97. https://doi.org/10.1007/s41109-021-00339-7

[16] Khodabandehlou, H., Pekcan, G., & Fadali, M. S. (2019). Vibration-based structural condition assessment using convolution neural networks. Structural Control and Health Monitoring, 26(2), e2308. https://doi.org/10.1002/stc.2308

[17] Sony, S., Gamage, S., Sadhu, A., & Samarabandu, J. (2022). Multiclass damage identification in a full-scale bridge using optimally tuned one-dimensional convolutional neural network. Journal of Computing in Civil Engineering, 36(2), 04021035. https://doi.org/10.1061/(ASCE)CP.1943-5487.0001035

[18] Chaabane, M., Mansouri, M., Ben Hamida, A., Nounou, H., & Nounou, M. (2019). Multivariate statistical process control-based hypothesis testing for damage detection in structural health monitoring systems. Structural Control and Health Monitoring, 26(1), e2287. https://doi.org/10.1002/stc.2287

[19] Zhang, S., Qiu, L., & Zeng, Z. (2026). Physics-Data Synergy in Structural Health Monitoring: A Multi-Scale Graph Contrastive Framework With Temperature-Adaptive Fusion. IEEE Access. https://doi.org/10.1109/ACCESS.2026.xxxxxx

[20] Piechnicki, F., Dos Santos, C. F., De Freitas Rocha Loures, E., & Dos Santos, E. A. P. (2021). Data fusion framework for decision-making support in reliability-centered maintenance. Journal of Industrial and Production Engineering, 38(1), 1–17. https://doi.org/10.1080/21681015.2020.1859722

[21] Tiboni, M., Remino, C., Bussola, R., & Amici, C. (2022). A review on vibration-based condition monitoring of rotating machinery. Applied Sciences, 12(3), 972. https://doi.org/10.3390/app12030972

[22] Kong, Q. Y., Rong, Y., Wang, G. L., Xu, Z. Q., Zhang, Q., Guan, Z. S., & Fan, Y. H. (2025). Adaptive Graph Neural Networks with Semi-Supervised Multi-Modal Fusion for Few-Shot Steel Strip Defect Detection. Processes, 13(11), 3520. https://doi.org/10.3390/pr13113520

[23] Noël, J. P., & Schoukens, M. (2019). Cross-fertilising research in nonlinear system identification between the mechanical, control and machine learning fields: Editorial statement. Mechanical Systems and Signal Processing, 130, 213–220. https://doi.org/10.1016/j.ymssp.2019.05.035

[24] Sarmadi, H., Entezami, A., & Daneshvar Khorram, M. (2020). Energy-based damage localization under ambient vibration and non-stationary signals by ensemble empirical mode decomposition and Mahalanobis-squared distance. Journal of Vibration and Control, 26(11–12), 1012–1027. https://doi.org/10.1177/1077546319898229

[25] Mousavi, M., & Gandomi, A. H. (2021). Prediction error of Johansen cointegration residuals for structural health monitoring. Mechanical Systems and Signal Processing, 160, 107847. https://doi.org/10.1016/j.ymssp.2021.107847

[26] Ping, W., Jiao, Y., Fan, H., & Zhang, X. (2026). Multimodal Fraud Detection in Financial Statements: A Trimodal Attention Network with Contrastive Evidence Chain Construction. IEEE Access. https://doi.org/10.1109/ACCESS.2026.xxxxxx

[27] Van Engelen, J. E., & Hoos, H. H. (2020). A survey on semi-supervised learning. Machine Learning, 109(2), 373–440. https://doi.org/10.1007/s10994-019-0587-0